Available online at www.sciencedirect.com
SCIENCE DIRECT®
Fluid Phase Equilibria 228–229 (2005) 479–485
FLUID PHASE EQUILIBRIA
www.elsevier.com/locate/fluid

Modeling vapor–liquid interfaces with the gradient theory in combination with the CPA equation of state☆

António J. Queimada[a,b], Christelle Miqueu[c], Isabel M. Marrucho[a], Georgios M. Kontogeorgis[b], João A.P. Coutinho[a,*]

[a] *Chemistry Department, CICECO, Aveiro University, 3810-193 Aveiro, Portugal*
[b] *Chemical Engineering Department, Engineering Research Center IVC-SEP, Technical University of Denmark, Building 229, DK-2800 Lyngby, Denmark*
[c] *UMR 5150 – Laboratoire des Fluides Complexes, Université de Pau et des Pays de L'Adour, B.P. 1155, Pau, Cedex 64013, France*

Abstract

With the final purpose of describing the important aqueous + hydrocarbon liquid–liquid interfaces, the gradient theory was combined with the Cubic-Plus-Association equation of state (CPA EOS), taking advantage of the correct representation of interfacial tensions provided by the gradient theory and the correct phase equilibrium of water + hydrocarbon systems already obtained from CPA.

In this work, preliminary studies involving the vapor–liquid interfacial tensions of some selected associating and non-associating pure components (water, ethanol, *n*-butane, *n*-pentane, *n*-hexane, *n*-heptane) are presented and discussed.

The good description of equilibrium properties such as vapor pressure and liquid and vapor phase densities is shown in the full range of the vapor–liquid saturation line. For non-associating components, results are compared with those from the Soave–Redlich–Kwong and Peng–Robinson equations of state.

A correlation for the influence parameter is presented from which surface tensions can be obtained in a broad temperature range with average errors smaller than 1%.

Keywords: CPA; Gradient theory; Hydrocarbon; Water; Interfacial tension; Model

1. Introduction

Fluid interfaces are important in several phenomena concerning phases at equilibrium. For example, aqueous interfaces are involved in processes such as extraction, distillation, adsorption or reaction and products such as coatings, paints, agrochemicals and detergents. For the petroleum industry, interfacial tensions are required for the design of the extraction process, as well as for the design of further operations taking place at the refinery. With the growing environmental concerns, interfacial tension gained increasing importance since it can determine the path, transport and fate mechanisms of organic pollutants in the environment. Despite its importance, there is still a considerable lack of experimental data and accurate models for its prediction.

Although very powerful for the description of interfacial tensions and density profiles across the interface, the gradient theory has not been widely used. Most of the proposed applications are limited to the liquid–vapor interface of some polar and non-polar fluids and simple mixtures [1–11]. Few authors [2,5,6,10] have attempted to model liquid–liquid interfaces and only recently associating equations of state such as the Associated-Perturbed-Anisotropic-Chain Theory (APACT) [5,6] or the Statistical-Associating-Fluid-Theory (SAFT) [10] were used for addressing liquid–liquid

☆ Paper presented at PPEPPD 2004 – 10th International Conference on Properties and Phase Equilibria for Product and Process Design.

* Corresponding author. Tel.: +351 234 401 507; fax: +351 234 370 084.
E-mail address: jcoutinho@dq.ua.pt (J.A.P. Coutinho).

0378-3812/$ – see front matter © 2004 Elsevier B.V. All rights reserved.
doi:10.1016/j.fluid.2004.08.011

interfacial tensions of systems containing associating components.

Since the gradient theory is based on the knowledge of the equilibrium phase densities and the Helmholtz free energy density calculated from equations of state, an association state-of-the-art thermodynamic model, the CPA EOS, which combines a physical contribution from a cubic EOS with an association contribution derived from Wertheim theory, will be used. This EOS has already shown to be an accurate model to describe the VLE and LLE of mixtures containing water, alkanes and alcohols [12–17]. Particularly for water + alkane systems, APACT, SAFT and CPA provide acceptable results for both the solubility of water in the hydrocarbon-phase and the hydrocarbon solubility in the aqueous phase [13,15,18–20]. APACT and SAFT have already been incorporated in the gradient theory framework [5,6,9–11]. This work presents the first results on the coupling with the CPA EOS.

In this paper, preliminary results involving the study of liquid–vapor interfaces of pure components will be presented and discussed. For the non-associating components chosen for this work, two cubic equations of state (EOS), the Soave–Redlich–Kwong (SRK) [21] and the Peng–Robinson (PR) [22] were selected for evaluation along with the CPA equation of state.

2. Model

2.1. Gradient theory

The gradient theory of fluid interfaces originated from the work of van der Waals, but only after Cahn and Hilliard [23] found its widespread use. Since 1958 it has been applied for the modeling of the liquid–vapor and liquid–liquid interfacial tension of different systems such as polar and non-polar fluids and some polymers. Recently, Miqueu generalized the gradient theory for multicomponent mixtures [1,8]:

$$\sigma = \int_{n_N^{\text{vap.}}}^{n_N^{\text{liq.}}} \sqrt{2\Delta\Omega(n) \sum_i \sum_j c_{ij} \frac{\mathrm{d}n_i}{\mathrm{d}n_N} \frac{\mathrm{d}n_j}{\mathrm{d}n_N}}\, \mathrm{d}n_N \tag{1}$$

$$\Delta\Omega(n) = \Omega(n) - P \tag{2}$$

where P is the equilibrium pressure (Pa), σ the surface tension (N m^{-1}), $n^{\text{liq.}}$ and $n^{\text{vap.}}$ the liquid and vapor phase densities, respectively (mol m^{-3}), subscript N the mixture reference component and c the so-called influence parameter (J m^5 mol^{-2}). $\Omega(n)$ is the grand thermodynamic potential defined as follows:

$$\Omega(n) = f_0(n) - \sum_i n_i \mu_i \tag{3}$$

where $f_0(n)$ is the Helmholtz free energy density of the homogeneous fluid, at local composition n, and μ_i are the pure-component chemical potentials.

The pure-component influence parameter, c_{ii}, has a theoretical definition, but this can hardly be implemented. For practical purposes, after the phase equilibrium is determined, the influence parameter is adjusted from surface tension data [1–11]:

$$c_{ii} = \frac{1}{2}\left[\frac{\sigma_{\text{exp.}}}{\int_{n^{\text{vap.}}}^{n^{\text{liq.}}} \sqrt{\Delta\Omega(n)}\, \mathrm{d}n}\right]^2 \tag{4}$$

The influence parameter should diverge close to the critical point, where surface tension vanishes.

For mixtures, cross influence parameters, c_{ij}, are calculated from the pure component influence parameters using a geometric mean rule:

$$c_{ij} = \sqrt{c_{ii} c_{jj}} \tag{5}$$

2.2. The CPA equation of state

Before using the gradient theory, it is necessary to determine the equilibrium densities of the coexisting phases, the chemical potentials and the Helmholtz free energy from an adequate model. In this work, the Cubic-Plus-Association (CPA) equation of state was used for these purposes. CPA is an equation of state that combines a physical contribution accounting for physical forces and an association contribution accounting for hydrogen bonding and other chemical forces [12–17]. Written in terms of the compressibility factor:

$$Z = Z^{\text{phys.}} + Z^{\text{assoc.}} \tag{6}$$

For the physical part the Peng–Robinson [17] or the Soave–Redlich–Kwong (SRK) terms can be used, with the last one being usually employed [12–16]:

$$Z^{\text{phys.}} = Z^{\text{SRK}} = \frac{V}{V-b} - \frac{a}{RT(V+b)} \tag{7}$$

The energy parameter, a, can be calculated as a function of temperature (Eq. (8)), where a_0 and c_1, fitted from vapor pressures and liquid densities, are used instead of the critical constants, allowing for better liquid density estimates and thus, no further need for a volume correction. The co-volume, b, is simultaneously optimized with a_0 and c_1.

$$a = a_0[1 + c_1(1 - \sqrt{T_{\text{r}}})]^2 \tag{8}$$

where $T_{\text{r}} = T/T_{\text{c}}$ stands for reduced temperature.

The pure component association contribution in CPA is similar with the one used in SAFT, written below using the Michelsen–Hendriks formalism [24]:

$$Z^{\text{assoc.}} = -\frac{1}{2}\left(1 + \rho \frac{\partial \ln g}{\partial \rho}\right) \sum_A (1 - X_A) \tag{9}$$

where ρ is the density, g the simplified radial distribution function and X_A the fraction of pure component not bonded at site A. For non-associating fluids, such as hydrocarbons, the association term disappears and CPA reduces to SRK.

A simplified version of the hard-sphere radial distribution function, proposed by Elliot et al. [25] and already used in CPA was employed [16]:

$$g(\rho) = \frac{1}{1 - 1.9\eta}, \quad \eta = \frac{1}{4}b\rho \tag{10}$$

where η is the packing fraction of hard spheres and b the co-volume, as calculated from the CPA cubic term.

X_A is found by solving the following equation, where A and B represent the different associating sites in the molecule:

$$X_A = \frac{1}{1 + \rho\sum_B X_B \Delta^{AB}} \tag{11}$$

where Δ^{AB} is the association strength between sites A and B on the associating molecule (self-association). For water, the 4C association scheme is selected, in which it is consider that hydrogen bonding occurs between the two hydrogen atoms and the two lone pairs of electrons in the oxygen of the water molecules.

$$X_A = X_B = X_C = X_D = \frac{-1 + \sqrt{1 + 8\rho\Delta^{AC}}}{4\rho\Delta^{AC}} \tag{12}$$

$$\Delta^{AA} = \Delta^{AB} = \Delta^{BB} = \Delta^{CC} = \Delta^{CD} = \Delta^{DD} = 0,$$
$$\Delta^{AC} = \Delta^{AD} = \Delta^{BC} = \Delta^{BD} \neq 0 \tag{13}$$

where Δ^{AC} is given by the expression:

$$\Delta^{AC} = g(\rho)\left[\exp\left(\frac{\varepsilon^{AC}}{RT}\right) - 1\right] b\beta^{AC} \tag{14}$$

ε^{AC} and β^{AC} are, respectively, the association energy and volume between sites A and C, and must be regressed together with the parameters of the physical part from experimental vapor pressure and liquid density data.

For ethanol, the 2B association scheme applies, where hydrogen bonding is considered between the hydroxyl hydrogen and one of the lone pairs of electrons from the oxygen atom in another alcohol molecule:

$$X_A = X_B = \frac{-1 + \sqrt{1 + 4\rho\Delta^{AB}}}{2\rho\Delta^{AB}} \tag{15}$$

$$\Delta^{AA} = \Delta^{BB} = 0, \qquad \Delta^{AB} \neq 0 \tag{16}$$

3. Results and discussion

In order to evaluate the performance of the combination of the gradient theory with the CPA EOS, a preliminary evaluation was carried out for some n-alkanes, an alcohol (ethanol) and water. For the n-alkanes, CPA is reduced to the physical contribution, thus allowing us to compare the results obtained from the physical term of CPA, where fitted a and b parameters are used (Table 1), with the a and b expressions used in SRK and PR. The required critical properties and acentric factors were collected from Ambrose and Tsonopoulos [26] and Magoulas and Tassios [27].

Table 1
CPA parameters for the pure components selected for this work (SI units)

	a_0	c_1	b ($\times 10^5$)	ε	β
n-C_4H_{10}	1.3143	0.7077	7.21	–	–
n-C_5H_{12}	1.8198	0.7986	9.10	–	–
n-C_6H_{14}	2.3678	0.8308	10.79	–	–
n-C_7H_{16}	2.9178	0.9137	12.54	–	–
H_2O	0.12277	0.6736	1.45	16655	0.0692
C_2H_5OH	0.86716	0.7369	4.91	21532	0.0080

Table 2
Modeling results in the reduced pressure range $0.45 < T_r < 0.80$

	EOS	%AAD[a]			
		P	$\rho_{liq.}$	$\rho_{vap.}$	σ
C_4H_{10}	CPA	0.44	4.56	1.42	0.06
	SRK	1.82	7.20	2.00	0.14
	PR	1.27	4.84	1.40	0.16
C_5H_{12}	CPA	0.46	0.77	1.26	0.08
	SRK	1.87	9.15	2.09	0.20
	PR	1.69	2.59	1.91	1.21
C_6H_{14}	CPA	2.25	0.75	3.15	0.21
	SRK	1.46	10.9	1.77	0.31
	PR	2.25	0.81	2.48	0.20
C_7H_{16}	CPA	1.61	0.51	2.53	0.22
	SRK	1.49	12.3	1.92	0.20
	PR	2.50	1.03	2.84	0.29
H_2O	CPA	0.73	0.82	1.72	0.27
C_2H_5OH	CPA	1.39	0.43	1.10	0.24

[a] $\%AAD = [(X_{calc.} - X_{model})/X_{calc.}] \times 100$.

Highly accurate data from the *NIST Chemistry WebBook* [28] was selected to obtain the n-alkane data on vapor pressure, saturation liquid and vapor phase densities and surface tension along the saturation curve.

As can be seen from Table 2 and Figs. 1 and 2 very good vapor pressure and vapor density results are obtained from CPA for the selected n-alkanes. Higher deviations are obtained close to the critical point, as could be expected [15].

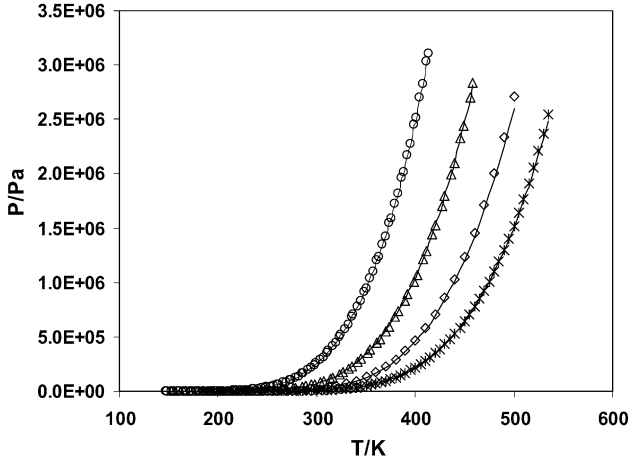

Fig. 1. n-Alkane vapor pressures. Experimental (◯, n-C_4H_{10}; △, n-C_5H_{12}; ◇, n-C_6H_{14}; ×, n-C_7H_{16}) and CPA results (—).

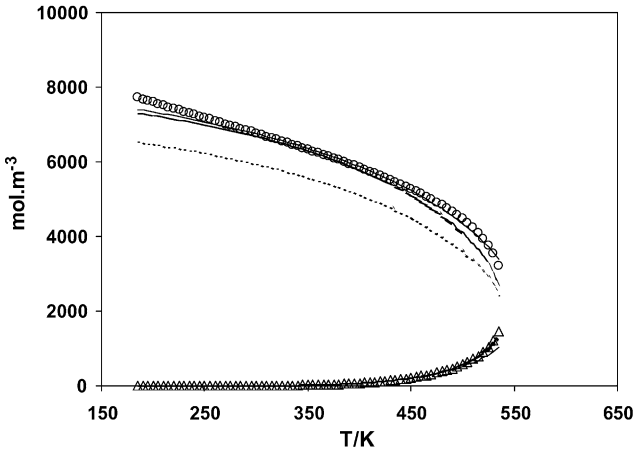

Fig. 2. *n*-Heptane saturation densities. Experimental (◯, liquid; △, vapor), CPA (—), SRK (- - -) and PR (– – –) estimates.

Still, results are better or within those obtained from the SRK or the PR EOS. Considerable improvements can be found with CPA on the equilibrium liquid phase densities, as can be seen in Fig. 2. Limitations on the use of classical cubic EOS for the estimation of liquid phase densities are known, and a regular procedure to overcome this problem is to include a volume translation as suggested by Peneloux et al. [29]. This procedure was already used by Miqueu [1,7,8] to obtain the correct liquid densities to use within the gradient theory. As can be seen in Table 2 and Figs. 1 and 2, the use of fitted parameters to correlate *a* and *b* on the physical term of CPA allows us to reproduce both liquid and vapor phase properties with a good accuracy with no need for a volume translation.

For the associating components water and ethanol data was collected from [28] (water) and from the correlations presented by Dillon and Pennoncello [30] and from the DIPPR database [31] (ethanol). As can be seen from Figs. 3–6 and Table 2, very good vapor pressure and equilibrium vapor and liquid phase densities are obtained both for water and ethanol.

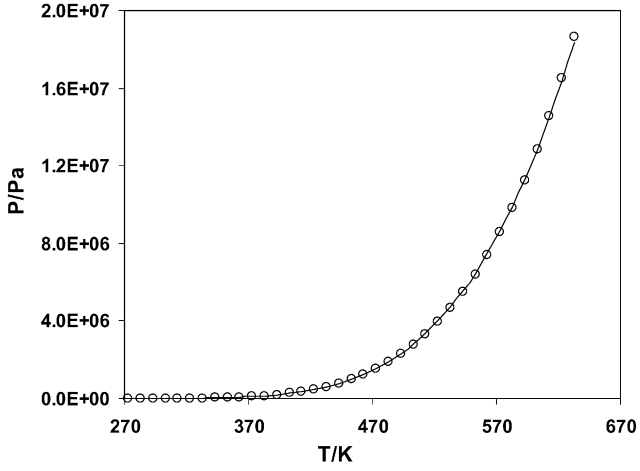

Fig. 3. Water vapor pressure: experimental (◯) and CPA results (—).

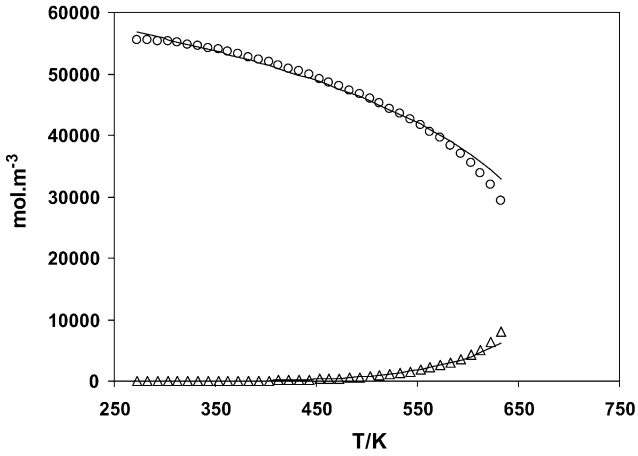

Fig. 4. Water density. Experimental (◯, liquid; △, vapor) and CPA (—) estimates.

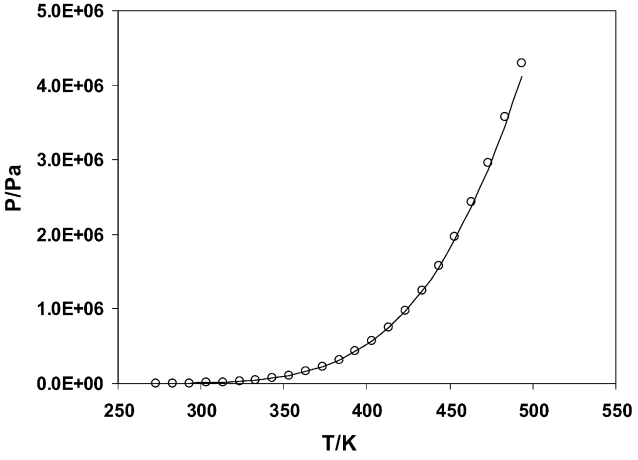

Fig. 5. Ethanol vapor pressure. Experimental (◯) and CPA results (—).

Using Eq. (4) the pure component influence parameters can be computed. These are plotted as $c/ab^{2/3}$ for *n*-heptane, water and ethanol in Figs. 7–9 as a function of $1 - T/T_c$. As can be seen in Fig. 7 for *n*-heptane, the three EOS present the

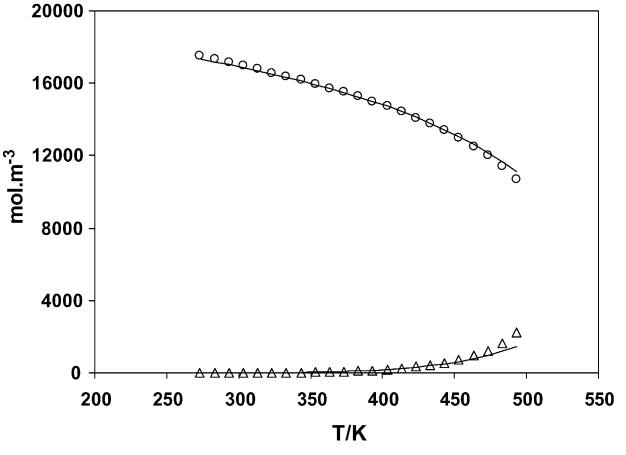

Fig. 6. Ethanol density. Experimental (◯, liquid; △, vapor) and CPA (—) estimates.

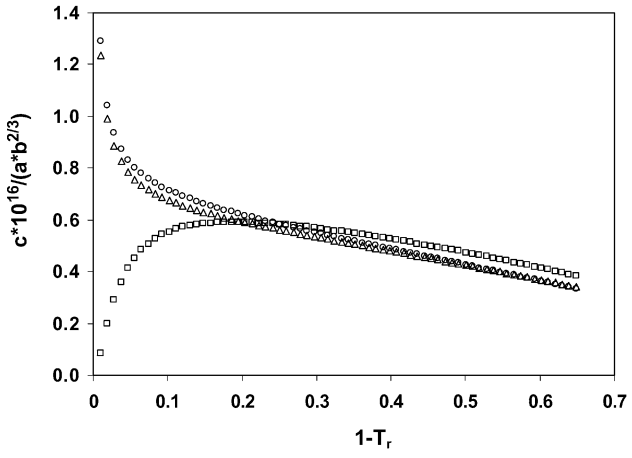

Fig. 7. *n*-Heptane influence parameters. CPA (□), SRK (◯) and PR (△) estimates.

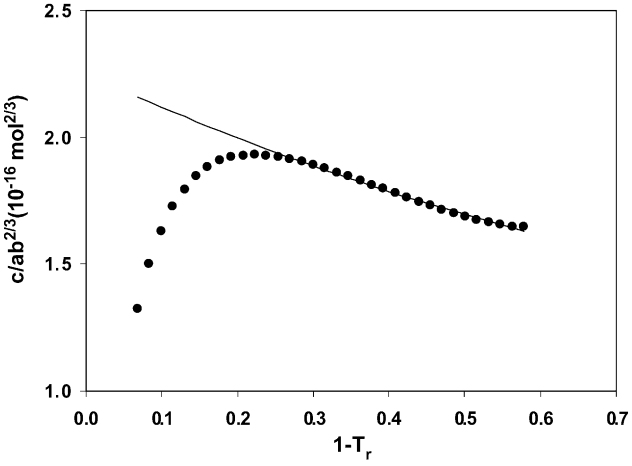

Fig. 8. Water influence parameters. CPA estimates (●) and correlation (—).

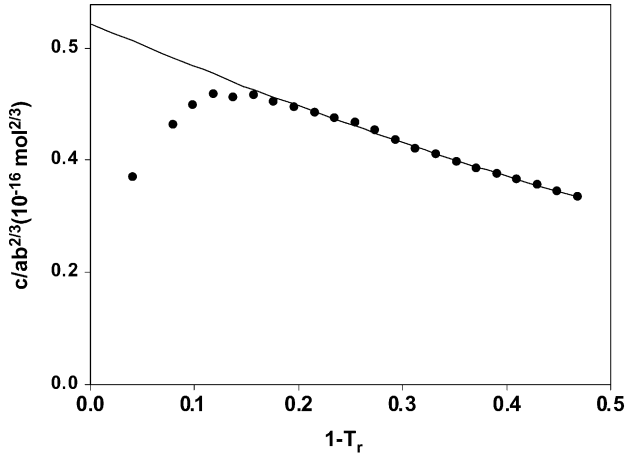

Fig. 9. Ethanol influence parameters. CPA estimates (●) and correlation (—).

Table 3
Correlation coefficients for calculating the influence parameters (Eq. (17))

Fluid	*D*	*E*	*F*
C_4H_{10}	0.7081	−0.0102	−0.5626
C_5H_{12}	0.7847	−0.3962	−0.3256
C_6H_{14}	0.6010	0.1349	−0.6887
C_7H_{16}	0.6266	−0.0539	−0.4986
H_2O	2.2505	−1.3646	0.5113
C_2H_5OH	0.5703	−0.7017	0.2471

same behavior in the $1 - T_r$ range above 0.2, but for CPA the behavior close to the critical point is exactly the opposite of what is found for SRK or PR. This qualitative trend is not in agreement with the theoretical definition of the influence parameter and the scaling laws near the critical point [1], and should be the consequence of having, while fitting the influence parameter, two different critical temperatures: one given by the CPA EOS and a second one implicit on the experimental surface tension data used for the fitting (that is, when $\sigma = 0$). This topic shall be further studied in the future.

Since it is known that SRK, PR and CPA cannot adequately represent the critical region and since for most of the practical purposes, the temperature range of interest will be in the $1 - T_r$ range above 0.2, a polynomial correlation can be proposed for the CPA influence parameter in order to obtain a fast estimate of the interfacial tension. As proposed by Miqueu [1,7,8] a linear correlation for $c/ab^{2/3}$ as a function of $1 - T_r$ is sufficient for the modeling of interfacial tensions when using a cubic EOS, but as can be observed from Figs. 7–9, a quadratic correlation seems more appropriate while using CPA, especially for water:

$$\frac{c}{ab^{2/3}} = D + E(1 - T_r) + F(1 - T_r)^2 \quad (17)$$

Correlation coefficients for the fluids selected for this work are presented in Table 3.

Surface tension was calculated using these coefficients in Eq. (17). Results are presented in Table 2 in the reduced

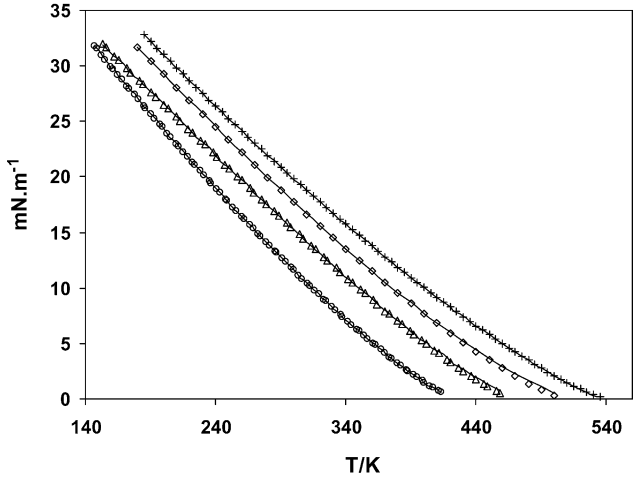

Fig. 10. *n*-Alkane surface tension. Experimental (◯, *n*-C_4H_{10}; △, *n*-C_5H_{12}; ◇, *n*-C_6H_{14}; +, *n*-C_7H_{16}) and gradient theory results (—).

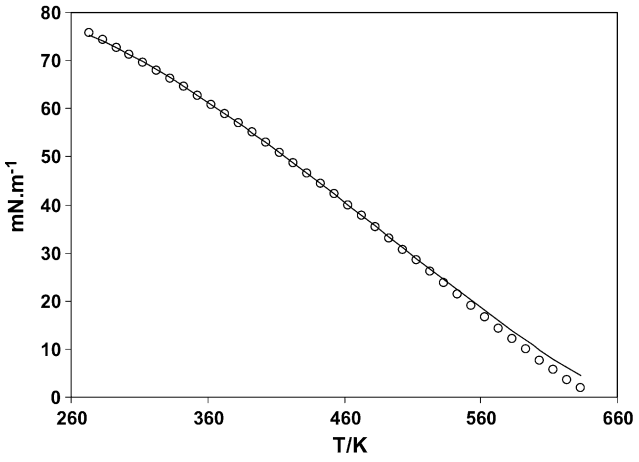

Fig. 11. Water surface tension. Experimental (◯) and gradient theory results (—).

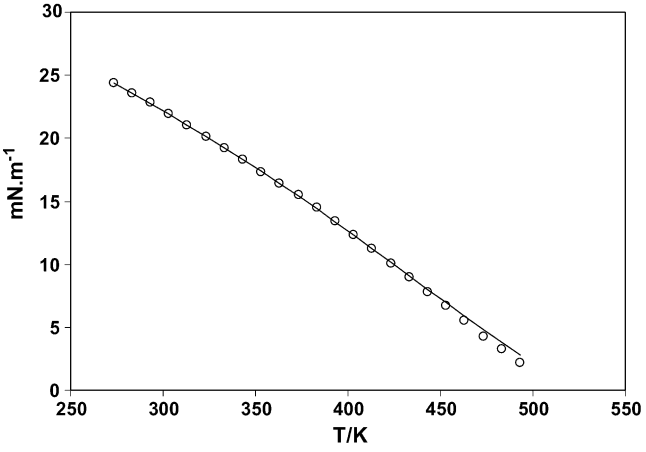

Fig. 12. Ethanol surface tension. Experimental (◯) and gradient theory results (—).

temperature range $0.45 < T_r < 0.8$ and Figs. 10–12. Very good results are obtained, as presented in Table 2 with average percent deviations below 1.2%. At higher temperatures, closer to the critical point, deviations are higher as already expected from the simplifications introduced with Eq. (17), but as can be seen from Figs. 10–12 the correct qualitative trend is present along all the results.

Based on these results, future developments will include extension of the theory to heavier *n*-alkanes, some aromatics and other associating components. Then, multicomponent mixtures and real fluids with a vapor–liquid or with a vapor–liquid and a liquid–liquid interface will be considered.

4. Conclusions

The correct volumetric and phase behavior resulting from the CPA EOS was presented and discussed in order to evaluate the use of this equation of state in the framework of the gradient theory of fluid interfaces. Using correlations to obtain the cubic and associative term pure component parameters, it was found that the saturated liquid phase densities could be obtained with a high accuracy with no need to perform any volume correction as usually needed while using cubic EOS with energy and co-volume parameters calculated from critical properties.

Highly accurate data on pure water, *n*-butane, *n*-pentane, *n*-hexane, *n*-heptane and ethanol were selected to calculate the pure component gradient theory influence parameters and from these a quadratic correlation was proposed from which surface tension can be obtained in the reduced temperature range below 0.8 with average errors of less than 1.5%. Although this correlation was presented for a limited range of reduced temperatures, it was found that qualitative results could be obtained in the full liquid range for the selected components evaluated on this work.

Future developments will focus on mixtures.

List of symbols

a	energy parameter in the physical term
a_0, c_1	parameters for calculating a (Eq. (8))
b	co-volume
c	influence parameter
D, E, F	correlation coefficients for the influence parameter (Eq. (17))
f_0	Helmholtz free energy density
g	radial distribution function (Eq. (10))
n	mole density
N	mixture reference component (Eq. (1))
P	vapor pressure
R	gas constant
T	temperature
V	volume
x	mole fraction
X_A	fraction of molecule not bonded at site A
Z	compressibility factor

Greek symbols

β	association volume
ε	association energy
Δ	association strength
η	reduced fluid density
μ	chemical potential
ρ	mole density
σ	surface tension
Ω	grand thermodynamic potential

Subscripts

c	critical
exp.	experimental
i, j	pure component indexes
liq.	liquid
r	reduced
vap.	vapor

Superscripts

assoc.	association
phys.	physical

Acknowledgements

A.J. Queimada thanks *Fundação para a Ciência e a Tecnologia* his Ph.D. scholarship BD/954/2000 and *Fundação Luso-Americana para o Desenvolvimento* for a conference scholarship. Samer O. Derawi is acknowledged for the discussions on the CPA EOS.

References

[1] C. Miqueu, Ph.D. Thesis, Univ. Pau et des Pays de L'Adour, Pau, France, 2000.
[2] Y.X. Zuo, E.H. Stenby, In Situ 22 (2) (1998) 157–180.
[3] Y.X. Zuo, E.H. Stenby, Fluid Phase Equilib. 132 (1–2) (1997) 139–158.
[4] P.M.W. Cornelisse, C.J. Peters, J.D. Arons, Fluid Phase Equilib. 117 (1–2) (1996) 312–319.
[5] P.M.W. Cornelisse, Ph.D. Thesis, Delft University of Technology, Delft, The Netherlands, 1997.
[6] P.M.W. Cornelisse, M. Wijtkamp, C.J. Peters, J. de Swaan Arons, Fluid Phase Equilib. 150–151 (1998) 633–640.
[7] C. Miqueu, B. Mendiboure, A. Graciaa, J. Lachaise, Fluid Phase Equilib. 207 (2003) 225–246.
[8] C. Miqueu, B. Mendiboure, A. Graciaa, J. Lachaise, Fluid Phase Equilib. 218 (2004) 189–203.
[9] H. Kahl, S. Enders, Fluid Phase Equilib. 172 (2000) 27–42.
[10] H. Kahl, S. Enders, Phys. Chem. Chem. Phys. 4 (2002) 931–936.
[11] J.C. Pàmies, Ph.D. Thesis, Universitat Rovira et Virgili, Tarragona, Spain, 2003.
[12] G.M. Kontogeorgis, E.C. Voutsas, I.V. Yakoumis, D.P. Tassios, Ind. Eng. Chem. Res. 35 (11) (1996) 4310–4318.
[13] I.V. Yakoumis, G.M. Kontogeorgis, E.C. Voutsas, E.M. Hendriks, D.P. Tassios, Ind. Eng. Chem. Res. 37 (10) (1998) 4175–4182.
[14] S.O. Derawi, Ph.D. Thesis, Technical University of Denmark, Lyngby, Denmark, 2002.
[15] E.C. Voutsas, G.C. Boulougouris, I.G. Economou, D.P. Tassios, Ind. Eng. Chem. Res. 39 (2000) 797–804.
[16] G.M. Kontogeorgis, I.V. Yakoumis, H. Meijer, E.M. Hendriks, T. Moorwood, Fluid Phase Equilib. 158–160 (1999) 201–209.
[17] J. Wu, J.M. Prausnitz, Ind. Eng. Chem. Res. 37 (1998) 1634–1643.
[18] F. Blas, Ph.D. Thesis, Universitat Rovira et Virgili, Tarragona, Spain, 2000.
[19] C. McCabe, A. Galindo, P.T. Cummings, J. Phys. Chem. B 107 (2003) 12307–12314.
[20] I.G. Economou, M.D. Donohue, Ind. Eng. Chem. Res. 31 (1992) 2388–2394.
[21] G. Soave, Chem. Eng. Sci. 27 (6) (1972) 1197–1203.
[22] D.Y. Peng, D.B. Robinson, Ind. Eng. Chem. Fund. 15 (1974) 59–64.
[23] J.W. Cahn, J.E. Hilliard, J. Chem. Phys. 28 (1958) 258–267.
[24] M.L. Michelsen, E.M. Hendriks, Fluid Phase Equilib. 180 (2001) 165–174.
[25] J.R. Elliot, S.J. Suresh, M.D. Donohue, Ind. Eng. Chem. Res. 29 (1990) 1476–1485.
[26] D. Ambrose, C. Tsonopoulos, J. Chem. Eng. Data 40 (1995) 531–536.
[27] K. Magoulas, D.P. Tassios, Fluid Phase Equilib. 56 (1990) 119–140.
[28] NIST Chemistry WebBbook, http://webbook.nist.gov/chemistry/fluid/.
[29] A. Peneloux, E. Rauzy, R. Freze, Fluid Phase Equilib. 8 (1982) 7–23.
[30] H.E. Dillon, S.G. Pennoncello, Int. J. Therm. 25 (2) (2004) 321–335.
[31] Design Institute for Physical Property Data, DIPPR Database, AIChE, New York, 1998.